Development 140, 205-215 (2013) doi:10.1242/dev.085423

Competition among gene regulatory networks imposes order within the eye-antennal disc of *Drosophila*

Bonnie M. Weasner and Justin P. Kumar*

SUMMARY

The eye-antennal disc of *Drosophila* gives rise to numerous adult tissues, including the compound eyes, ocelli, antennae, maxillary palps and surrounding head capsule. The fate of each tissue is governed by the activity of unique gene regulatory networks (GRNs). The fate of the eye, for example, is controlled by a set of fourteen interlocking genes called the retinal determination (RD) network. Mutations within network members lead to replacement of the eyes with head capsule. Several studies have suggested that in these instances all retinal progenitor and precursor cells are eliminated via apoptosis and as a result the surrounding head capsule proliferates to compensate for retinal tissue loss. This model implies that the sole responsibility of the RD network is to promote the fate of the eye. We have re-analyzed *eyes absent* mutant discs and propose an alternative model. Our data suggests that in addition to promoting an eye fate the RD network simultaneously functions to actively repress GRNs that are responsible for directing antennal and head capsule fates. Compromising the RD network leads to the inappropriate expression of several head capsule selector genes such as *cut*, *Lim1* and *wingless*. Instead of undergoing apoptosis, a population of mutant retinal progenitors and precursor cells adopt a head capsule fate. This transformation is accompanied by an adjustment of cell proliferation rates such that just enough head capsule is generated to produce an intact adult head. We propose that GRNs simultaneously promote primary fates, inhibit alternative fates and establish cell proliferation states.

KEY WORDS: Eyes absent, Sine oculis, Eye, Head capsule, Antenna, Cell proliferation, Gene regulatory network

INTRODUCTION

The identity of individual tissues and organs is specified during development by combinations of selector genes and signal transduction pathways that are organized into functional units called gene regulatory networks (GRNs) (Davidson and Levine, 2008). The eye-antennal disc of *Drosophila* provides an opportunity to understand the mechanisms by which multiple GRNs function within a single tissue to establish regional identities. This monolayer epithelium, which is derived from an eight- to nine-cell embryonic clone, gives rise to the adult compound eyes, the ocelli, the antennae, maxillary palps and surrounding head cuticle (Vogt, 1946; Ferris, 1950; Gehring, 1966; Ouweneel, 1970; Baker, 1978; Madhavan and Schneiderman, 1977; Haynie and Bryant, 1986). A potential mechanism for specification of distinct regions of the disc relies on compartmentalization of selector gene expression and activity starting at the earliest stages of development. However, in the eye-antennal disc this model is unlikely to be an accurate summary as the GRNs that govern distinct adult structures are expressed in overlapping patterns within the early disc primordium. During the first and early second larval instar, several genes that regulate specification of the retina, antenna and surrounding head capsule are simultaneously expressed throughout the entire eye-antennal primordium (Quiring et al., 1994; Royet and Finkelstein, 1996; Czerny et al., 1999; Kumar and Moses, 2001a; Kumar and Moses, 2001b; Jang et al., 2003; Aldaz et al., 2003). By the late second instar, the expression patterns of the antennal and retinal GRNs are segregated to the anterior and posterior sections of the epithelium, respectively (Kumar and Moses, 2001a; Kenyon et al., 2003). The mechanisms that lead to this initial segregation of GRNs are poorly understood. Two alternative models can account for the maintenance of these segregated gene expression patterns. In the first, the asymmetry in GRN expression patterns and levels is maintained and amplified solely via internal self-reinforcing transcriptional feedback loops. In the second, the mutually exclusive transcriptional patterns of distinct GRNs are preserved by both internal transcriptional activation and reciprocal repression of each other's expression.

In this article, we investigate these models by examining the developmental effects of compromising the retinal determination (RD) network. This network comprises a set of genes that together promote formation of the eye in all seeing animals (Halder et al., 1995; Callaerts et al., 1997). Deletion of eye-specific enhancer elements within the regulatory regions of the *eyeless* (*ey*), *eyegone* (*eyg*), *sine oculis* (*so*), *eyes absent* (*eya*) and *dachshund* (*dac*) genes results in replacement of the compound eyes with head capsule tissue (Hoge, 1915; Milani, 1941; Bonini et al., 1993; Cheyette et al., 1994; Mardon et al., 1994; Quiring et al., 1994; Serikaku and O'Tousa, 1994; Jang et al., 2003). Studies of *so*, *eya* and *dac* mutants have led to differing conclusions regarding the molecular and developmental relationship between eye and head capsule fates. Results from studies of retinas that are completely mutant for either *so* or *eya* have suggested that all retinal progenitor and precursor cells are eliminated from the eye disc and that the surrounding head capsule proliferates and replaces the missing retinal tissue (Bonini et al., 1993; Pignoni et al., 1997). These results suggest that a non-autonomous signaling system exists. Indeed, a gradient of Wingless (Wg) signaling from the head capsule is thought to pattern parts of the peripheral retina (Tomlinson, 2003).

By contrast, studies of null *dac* and *so* clones demonstrated that, in certain instances, the mutant tissue is autonomously transformed

Department of Biology, Indiana University, Bloomington, IN 47405, USA.

*Author for correspondence (jkumar@indiana.edu)

Accepted 5 October 2012

into head capsule (Mardon et al., 1994; Salzer and Kumar, 2009). In these cases, cells mutant for *so* also express *cut*, which encodes an antennal and head capsule selector protein (Bodmer et al., 1987; Blochlinger et al., 1993; Salzer and Kumar, 2009). Consistent with these effects, loss of either *homothorax* (*hth*) or *extradenticle* (*exd*) within the head capsule leads to the formation of ectopic eyes (González-Crespo and Morata, 1995; Rauskolb et al., 1995; Pai et al., 1998; Pichaud and Casares, 2000). Likewise, overexpression within the eye field of *Arrowhead* (*Awh*), a LIM-type homeodomain transcription factor that is important for the formation of ventral head capsule, leads to replacement of the retina with head capsule (Curtiss and Heilig, 1995; Curtiss and Heilig, 1997; Roignant et al., 2010). The loss of retinal tissue is thought to be in part due to a block in retinal precursor cell formation and a downregulation of eye-promoting genes. Finally, downregulation of Wg signaling within the eye disc leads to precocious retinal development at the dorsal and ventral margins, whereas ectopic Wg activation in the eye disc leads to repression of RD genes and a conversion of the eye to head capsule (Ma and Moses, 1995; Treisman and Rubin, 1995; Baonza and Freeman, 2002). These results support the model in which individual gene regulatory networks (after being initially segregated) actively repress all other selector genes, thereby maintaining regional specificity.

Here, we show that in *eya* mutant eye discs a population of retinal progenitor and precursor cells survives a wave of developmental cell death. These cells go on to inappropriately express several non-retinal selector genes, a process that subsequently results in transformation of the eye field into head capsule. These effects were observed both in whole eye discs and in mutant clones. This switch in tissue fate is accompanied by an adjustment in the growth rate of the former eye disc. Instead of producing the number of cells that normally would have been needed to produce the compound eye, only the number of cells that is required to produce an intact adult head are generated. Attempts to restore growth rates by inhibiting developmental cell death and/or stimulating cell proliferation largely failed, suggesting that tissue fate is directly linked to cell proliferation levels. In summary, we show here that the RD network functions within the eye field primordium to promote formation of the retina and to inhibit the formation of head capsule simultaneously. We propose that regional specification of tissue fates is achieved through competition between selector gene networks.

MATERIALS AND METHODS

Fly strains

The following stocks were used: (1) eya^2; (2) so^1; (3) FRT42D so^3/CyO; (4) FRT40A eya^1/CyO; (5) FRT42D hpo^{3D}/CyO; (6) FRT42D Ubi-GFP/CyO; (7) FRT40A Ubi-GFP/CyO; (8) yweyflp; (9) UAS-p35; (10) UAS-eyg; (11) UAS-N^{ICD}; (12) UAS-Dl; (13) UAS-dpp; (14) UAS-tkv^{QD}; (15) UAS-hh; (16) UAS-$RasD^{V12}$; (17) UAS-bsk; (18) UAS-upd; (19) UAS-hop; (20) UAS-yki; (21) UAS-sd; (22) UAS-stg; (23) UAS-tsh; (24) UAS-tio; (25) ey-GAL4; (26) dpp-GAL4; (27) emc-GFP^{YB0067}; (28) mirr-lacZ. so^3, hpo^{D3} and eya^1 loss-of-function clones were generated by the following genotypes: (1) yweyflp; FRT42D so^3/FRT42D Ubi-GFP; (2) yweyflp; eya^2 FRT42D hpo^{D3}/eya^2 FRT42D Ubi-GFP; (3) yweyflp; FRT40A eya^1/FRT40A Ubi-GFP. All crosses were conducted at 25°C.

Antibodies and microscopy

The following antibodies were used: (1) mouse anti-Cut; (2) rat anti-Elav; (3) rabbit anti-Lim1; (4) mouse anti-Ey, (5) rabbit anti-Tsh; (6) guinea pig anti-Hth; (7) rabbit anti-Hth; (8) rabbit anti-CC3; (9) mouse anti-Exd; (10) mouse anti-Eya; (11) guinea pig anti-Otd; (12) mouse anti-Dac; (13) mouse anti-β-Gal; (14) chicken anti-β-Gal; (15) rabbit anti-PH3. Primary antibodies were obtained from Amit Singh (University of Daytona, OH, USA), Richard Mann (Columbia University Medical Center, NY, USA), Juan Botas (Baylor College of Medicine, Houston, TX, USA), Stephen Cohen (A*STAR, Singapore), Tiffany Cook (Cincinnati Children's Hospital, OH, USA), Abcam, Cell Signaling Technologies, Life Technologies and the Developmental Studies Hybidoma Bank. Secondary antibodies (donkey anti-mouse, goat anti-mouse, donkey anti-rat, goat anti-rabbit, donkey anti-rabbit, donkey anti-guinea pig and donkey anti-chicken) and phalloidin were obtained from Jackson Laboratories and Invitrogen. TUNEL staining was performed using the Roche In Situ Cell Death Detection Kit. Imaginal discs and adult flies were prepared as described by Anderson et al. (Anderson et al., 2012).

Determination of tissue growth and proliferation rates

Adult flies were allowed to lay eggs for 2 hours at 25°C. Individual eggs were placed in tubes containing fly media and allowed to age for varying numbers of hours at 25°C. Imaginal discs were dissected and stained with phalloidin in order to identify the outline of the eye and wing fields. Images of imaginal discs were imported into ImageJ and boundaries of discs were traced five times. The area (in pixels) was calculated and an average determined for each disc. Box plot analysis was conducted to remove outliers. Standard errors were calculated in Excel and an F-test was used to determine equal or unequal variance. If the F-value was greater than 0.05 then *P*-values were calculated using Student's *t*-test of equal variance. If the F-value was less than 0.05 then *P*-values were calculated using Student's *t*-test of unequal variance. Similar methods were used to calculate the wing size of freshly eclosed adults as well as the percentage of the eye disc that contained *dac*-positive cells. The area of the *dac*-positive tissue was divided by the area of the entire eye field. Proliferation rates were calculated by counting the number of pH3-positive cells (Cell Counter Plug-In within Image J) at different time points and dividing by the number of hours that separates the different time points. Because eya^2 discs lack a furrow, we only counted dividing cells ahead of the furrow in wild-type discs in order to keep comparisons equivalent.

RESULTS

Survival of retinal precursors and progenitors in eya^2 mutants

By the early third larval instar, distinct regions of the eye antennal disc that give rise to the retina, antenna and surrounding head capsule can be distinguished based on selector gene expression (supplementary material Fig. S1) (Kumar and Moses, 2001a; Kenyon et al., 2003). Cells that lie at the most anterior regions of the eye field and that border the antennal disc give rise to a portion of the surrounding head capsule and express *hth*, *exd*, *cut* (*ct*) and *Lim1* (Blochlinger et al., 1993; González-Crespo and Morata, 1995; Rauskolb et al., 1995; Pai et al., 1998; Pichaud and Casares, 2000; Tsuji et al., 2000). Cells adjacent to this zone co-express three RD genes: *teashirt* (*tsh*), *ey* and *hth* (Bessa et al., 2002). The encoded proteins form a trimeric complex that acts to inhibit the expression of several downstream RD genes, including *so*, *eya* and *dac*. As a result, these 'retinal progenitors cells' remain in a highly proliferative state and forestall differentiation (Bessa et al., 2002; Lopes and Casares, 2010; Peng et al., 2009). This block in differentiation is relieved as the morphogenetic furrow approaches. Hedgehog and Decapentaplegic signals from the furrow repress *hth* expression resulting in transcriptional activation of *so*, *eya* and *dac* (Bessa et al., 2002). These cells are now called retinal precursors, as they are competent to enter the morphogenetic furrow and give rise to all cells of the adult retina (Lebovitz and Ready, 1986).

Prior studies of *eya* loss-of-function mutants have suggested that all retinal progenitors and precursors are lost through apoptosis (Bonini et al., 1993). The implication is that the extra head capsule tissue seen in adult flies is due to overproliferation of the normal head capsule. We sought to re-examine the fate of retinal progenitor and precursor cells in the homozygous viable eya^2 mutant. This

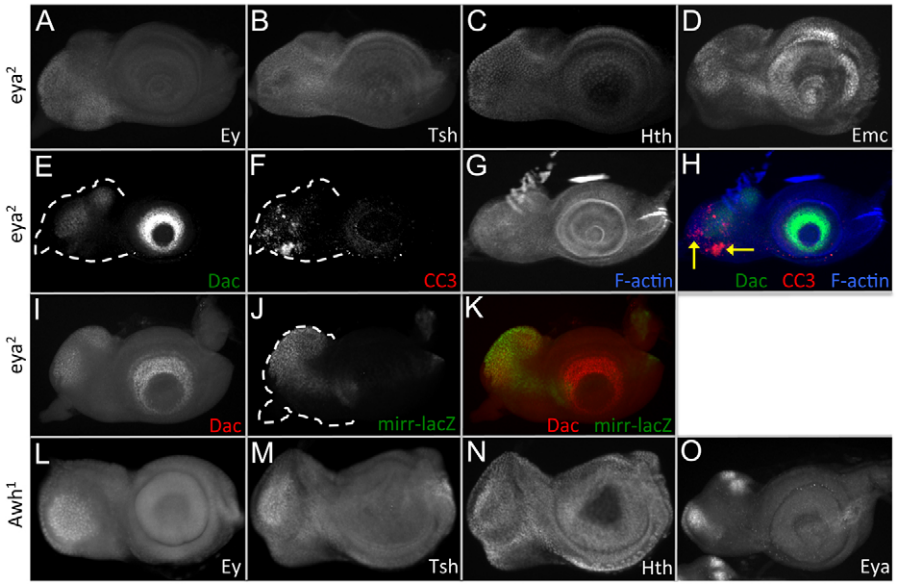

Fig. 1. A sub-population of retinal progenitor and precursor cells survive within the *eya*^{2} mutant eye field. (**A-O**) Confocal images of *Drosophila* third instar eye-antennal discs immunostained for the indicated proteins. Arrows in panel H denote areas that are CC3 positive but Dac negative. Dashed lines delineate the outline of the eye disc.

allele contains a 322-bp deletion that removes an eye-specific enhancer within the eya transcription unit (Bui et al., 2000). This results in the absence of both *eya* transcripts and Eya protein from the eye field. In the context of eye development, the *eya*^{2} mutant is a functional null allele. Using antibodies against Ey, Tsh and Hth proteins we find that a subset of progenitor cells do exist within the *eya*^{2} disc (Fig. 1A-C). These progenitors go on to become retinal precursor cells as we detect the continued presence of Dac, a transcriptional co-repressor and marker for this cell type (Fig. 1I; Fig. 7A) (Chen et al., 1997). Confirming that these Dac-positive cells are retinal precursors, we also detected *extra macrochaetae* (*emc*), which is normally enriched within retinal precursor cells just ahead of the morphogenetic furrow (Fig. 1D). We conclude that a subset of retinal precursors is present in the *eya*^{2} mutants.

In order to rule out the possibility that these retinal precursor cells are eliminated by apoptosis, we co-stained *eya*^{2} discs with antibodies that detect Dac and cleaved caspase-3 (CC3). The vast majority of *dac*-positive precursor cells in these discs do not undergo developmental cell death (Fig. 1E-H). We have used a *mirr-lacZ* line to show that the surviving cells appear to have a dorsal identity (Fig. 1I-K). These results suggest that in *eya*^{2} mutants a population of retinal progenitor and precursor cells survive and retain at least some characteristics of normal eye development. We propose that retinal progenitors/precursors within RD mutant eye fields will adopt a head capsule fate despite expressing several RD genes.

We draw support for this model from an analysis of *Arrowhead* (*Awh*) mutants. *Awh*^{1} is a gain-of-function allele characterized by replacement of the compound eyes with head capsule tissue, a phenotype that is identical to that of several RD loss-of-function mutants (Bonini et al., 1993; Cheyette et al., 1994; Serikaku and O`Tousa, 1994; Quiring et al., 1994; Curtiss and Heilig, 1995; Jang et al., 2003). Similar to these examples, *Awh*^{1} mutants are characterized by a dramatic reduction in the overall size of the disc and deficits in the expression of genes that regulate furrow progression and photoreceptor development (Curtiss and Heilig, 1995). It has been proposed that the loss of retinal tissue in *Awh*^{1} is due to a block in retinal precursor cell formation and not to developmental cell death as in *eya*^{2} mutants (Curtiss and Heilig, 1995). However, we were able to detect Ey, Tsh, Hth, Eya and Dac proteins (Fig. 1L-O; data not shown), indicating that retinal progenitors and precursors are present in this mutant. *Awh*^{1} represents an example in which cells of the eye disc express non-retinal gene regulatory network genes. This is sufficient to induce cells of the eye disc to adopt a head capsule fate.

Head capsule markers are present in retinal progenitor cells of *eya*^{2} mutants

Based on our analysis of *eya*^{2} and *Awh*^{1} mutants, we predict that the surviving retinal progenitor cells within the *eya*^{2} disc should undergo a cell fate switch and thus begin to express genes that are appropriate for a head capsule fate while continuing to express genes of the RD network. In order to test our model, we examined the expression of four genes that are known to play roles in head capsule development: *ct*, *orthodenticle* (*otd*; *oc* – FlyBase), *wg* and *Lim1* (Bodmer et al., 1987; Royet and Finkelstein, 1995; Royet and Finkelstein, 1996; Royet and Finkelstein, 1997; Tsuji et al., 2000; Kenyon et al., 2003; Tomlinson, 2003; Roignant et al., 2010).

Although *ey* is expressed within a broad zone ahead of the morphogenetic furrow its transcription is silenced in the swath of cells within the eye disc that borders the antennal disc (Fig. 2A, arrow) (Quiring et al., 1994). As previously stated, these anterior-most cells give rise to head capsule tissue (Haynie and Bryant, 1986) and express both *ct* and *Lim1* (Fig. 2B-D, arrows) (Blochlinger et al., 1993; Tsuji et al., 2000; Roignant et al., 2010). In normal development, Ey protein is not co-distributed with either of these two factors (Fig. 2A-C) and this has led to a model in which Ct and Lim1 repress *ey* transcription and vice versa (Kenyon et al., 2003; Roignant et al., 2010). We find that Ct and Lim1 proteins are found within the *eya*^{2} mutant eye disc (Fig. 2H-J) despite the continued presence of Ey (Fig. 2G) (Halder et al., 1998). In fact, Ey and Lim1 are co-expressed within many cells of the mutant disc (Fig. 2I, bracket). We were unable to confirm co-expression of Ey and Ct because the available antibodies are both generated in the same species. However, based on the images of individual antibody staining, we are confident that both proteins are expressed within the same sets of cells.

Our interpretation of the Ey and Lim1 colocalization pattern is that transcriptional repression of at least *Lim1* in the eye disc might actually be mediated by *so* and *eya*, both of which are known

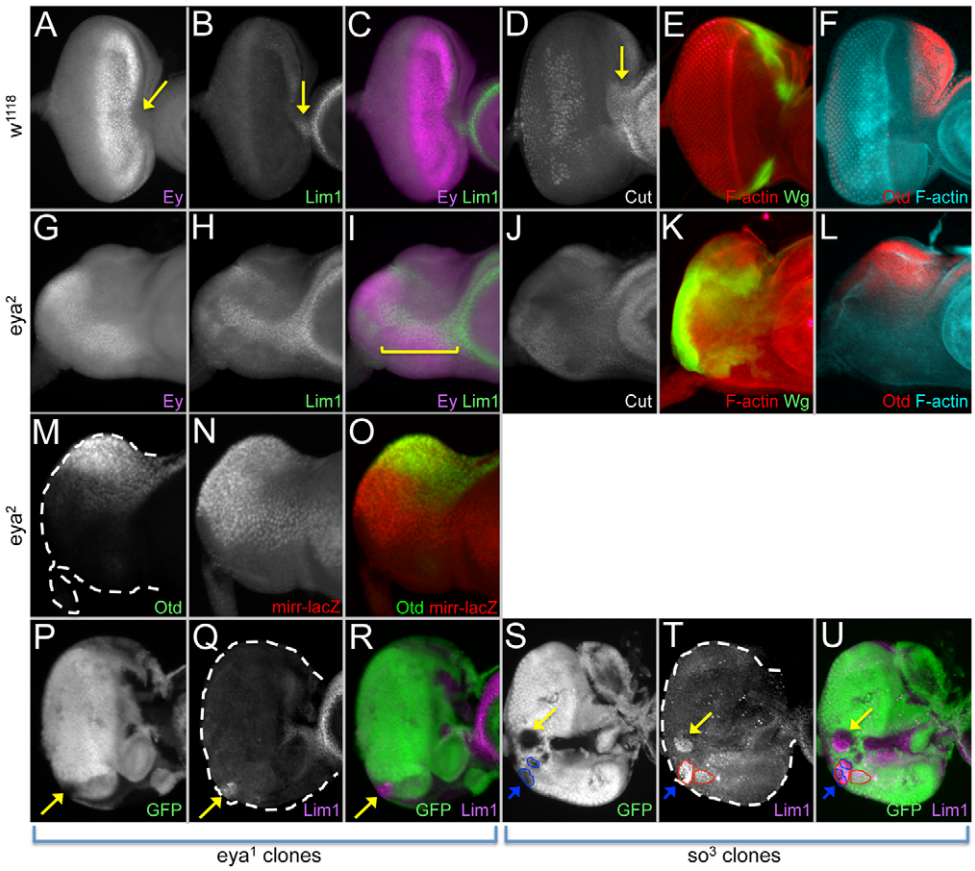

Fig. 2. Head capsule genes are de-repressed in *eya* and *so* mutant fields. (**A-U**) Confocal images of *Drosophila* third instar eye discs (antennal segments are not shown) immunostained for the indicated proteins. Bracket in panel I indicates areas in which Lim1 and Ey are co-expressed. Yellow and blue arrows mark examples of autonomous and non-autonomous induction of Lim1, respectively. Dashed lines delineate the outline of the eye disc.

downstream targets of *ey* (Halder et al., 1998; Niimi et al., 1999; Ostrin et al., 2006). To test this hypothesis, we generated so^3 and eya^1 loss-of-function clones in the eye and demonstrate that, in both cases, Lim1 was de-repressed within the clonal tissue (Fig. 2P-U, yellow arrows). We have also shown that *ct* transcription is de-repressed within so^3 clones (Salzer and Kumar, 2009). Interestingly we also find that *Lim1* de-repression is not limited to the clone (Fig. 2S-U, blue arrows). The non-autonomous activation of *Lim1* might be the result of signaling between mutant and wild-type sectors; however, the identity of the signaling mechanism is not known.

Wg signaling functions to specify the dorsal head (Royet and Finkelstein, 1996; Royet and Finkelstein, 1997; Baonza and Freeman, 2002) and is used reiteratively during retinal development first to prevent ectopic furrow initiation at the dorsal and ventral margins of the eye disc (Ma and Moses, 1995; Treisman and Rubin, 1995) and then to eliminate ommatidia from the periphery of the pupal eye (Tomlinson, 2003; Lin et al., 2004). Several prior studies have reported genetic interactions between *wg* and *eya*, although they have arrived at different conclusions. One study suggested that *eya* prevents *wg* expression within the eye disc (Hazelett et al., 1998) whereas two others have suggested that *eya* lies downstream of *wg* during retinal and ocelli specification (Baonza and Freeman, 2002; Blanco et al., 2009). We have examined *wg* transcription in eya^2 discs and our own analysis supports the conclusions of Hazelett and colleagues. In wild-type discs, high levels of *wg* transcription are observed at the margins of the eye field with small adjacent zones having lower *wg* levels (Fig. 2E). In eya^2 discs, high *wg* expression remains at the margins but we now observe a significantly larger area of the disc proper that contains lower levels of *wg* transcription (Fig. 2K). This is consistent with the de-repression of *wg* transcription that is observed in *eya* null mutant clones (Hazelett et al., 1998).

otd is a known target of Wg signaling and functions to specify the fates of photoreceptors, the ocelli and the dorsal vertex portion of the head capsule (Royet and Finkelstein, 1995; Royet and Finkelstein, 1996; Royet and Finkelstein, 1997; Tahayato et al., 2003; Blanco et al., 2009). Within the eye disc, this transcription factor is distributed within the dorsal-anterior quadrant and within a strip of cells along the dorsal edge of the antennal disc (Fig. 2F). Given the observed expansion of *wg*, *ct* and *Lim1* expression in eya^2 discs, we expected to see a similar expansion of Otd expression. However, *otd* transcription does not appear to expand in eya^2 mutant discs and continues to be restricted to its normal expression domain (Fig. 2L), thereby suggesting that the transformed retinal precursor cells are not fated to become dorsal head vertex. However, the precise sub-identity of the newly specified head capsule is not completely clear. Although most of the Otd-positive cells continue to express *mirr-lacZ*, a dorsal compartment marker (Fig. 2M-O), the pattern of de-repression and expansion of the other head capsule selector genes is variable, suggesting that the cell fate switch proceeds in a non-stereotyped manner. The variability in gene expression within the eye field results in an equally variable pattern of bristles in the adult head covering (supplementary material Fig. S2). We conclude that surviving retinal progenitor cells undergo a genomic switch in their transcriptional profiles resulting in transformation of the eye into head capsule.

Identification of growth and cell death phases in eya^2 mutant discs

We next set out to determine the critical developmental window at which growth in *eya* mutants differs from wild-type retinas and to

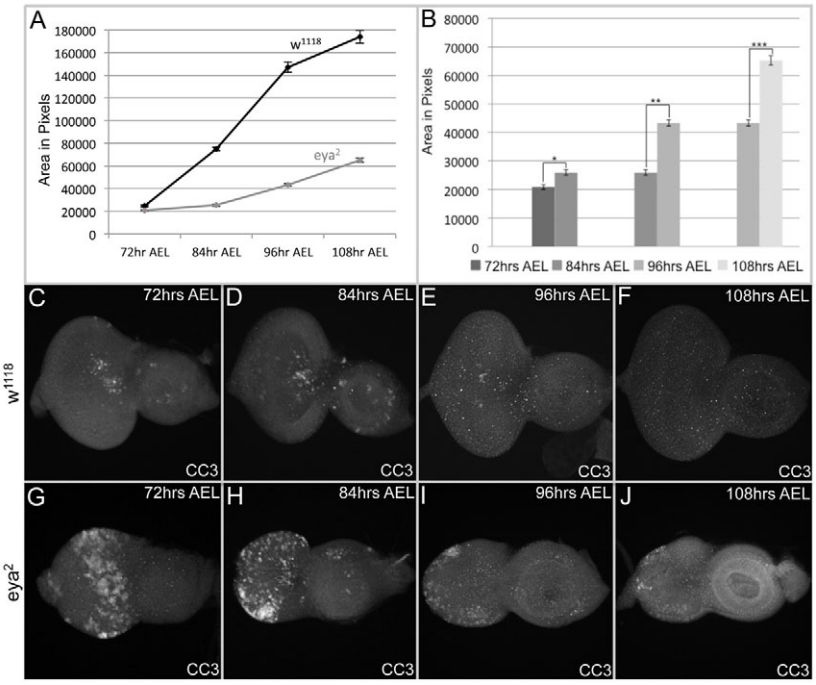

Fig. 3. Time course of growth deficits and increased cell death in *eya²* mutants. (**A**) Graph comparing the size of wild-type and *eya²* *Drosophila* eye fields at different times. Error bars represent xxx. (**B**) Graph comparing the size of *eya²* eye fields at different times. All *P*-values are statistically significant and are listed within supplementary material Table S1. **P*<0.05, ***P*<0.05, ****P*<0.05. Error bars represent s.e.m. (**C-J**) Confocal images of third instar eye-antennal discs immunostained for Cleaved Caspase-3 (CC3) at different times AEL.

identify the apoptotic phases. Eye-antennal discs from precisely staged individual wild-type and *eya²* larvae were dissected and the areas of the eye fields were determined. Statistically significant differences between the areas of wild-type and *eya²* retinal primordia could be seen as early as 72 hours after egg laying (AEL) (Fig. 3A). By this point in normal development, the expression patterns of several RD genes (including *eya*) are restricted to the eye field (supplementary material Fig. S1). The difference in the size of the eye fields of wild-type and *eya²* discs becomes more pronounced as development proceeds (Fig. 3A).

We then attempted to determine whether the massive levels of developmental cell death reported for *eya²* mutants (Bonini et al., 1993) temporally track with the differences that we have seen in the sizes of the eye fields. The highest levels of cell death occurs between 72 and 84 hours AEL (Fig. 3C,D,G,H) with limited levels of apoptosis being detected at either 96 or 108 hours AEL (Fig. 3E,F,I,J). The results from these experiments indicate that an epoch of cell death between 72 and 84 hours AEL affects the final size of the *eya²* disc. As Wg signaling has been show to induce cell death in the eye (Cordero et al., 2004; Cordero and Cagan, 2010; Lin et al., 2004; Lim and Tomlinson, 2006; Nicholson et al., 2009), it is a distinct possibility that the induction of *wg* expression is responsible for the elevated levels of cell death that we see in *eya²* discs. As the *eya²* discs remain smaller throughout the later stages of development, our data also suggests that cell proliferation rates are not elevated to compensate for the earlier apoptosis (see below). However, we do note that *eya²* discs continue to increase in size during the second and third instar larval stages (Fig. 3B), suggesting that at a later point in development the mutant eye field will require more cells than are present after the initial wave of developmental cell death.

eya² mutants exhibit a dynamic and transitory developmental delay in wing disc growth

Genetic or physical injury to individual imaginal discs delays the development and proliferation of other imaginal discs until the injured disc has been repaired (Hussey et al., 1927; Simpson et al., 1980; Smith-Bolton et al., 2009). In order to rule out the possibility that the differences that we see in the size of the eye disc are due to injury-induced global developmental delays, we examined the

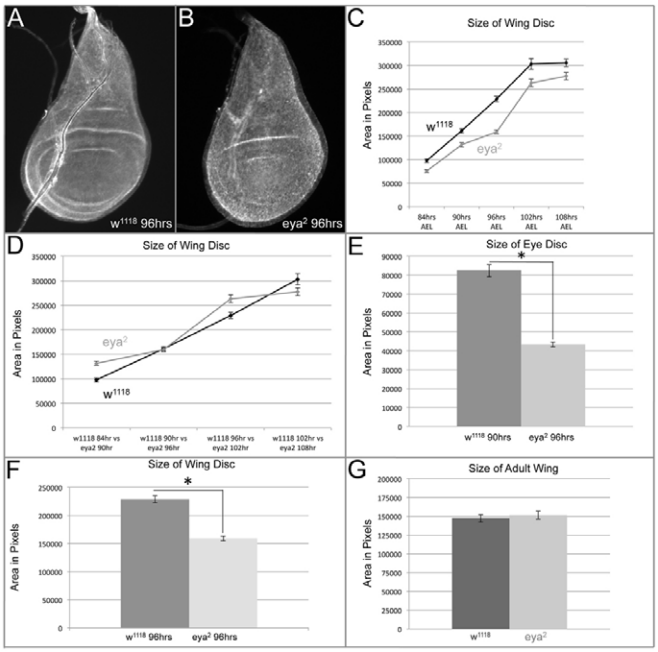

Fig. 4. Loss of *eya* causes a dynamic and transitory developmental delay. (**A**,**B**) Confocal images of *Drosophila* third instar wing discs immunostained for F-actin. (**C**) Graph comparing the size of wild-type and *eya²* wing discs at different times. (**D**) Graph comparing the size of wild-type and *eya²* wing discs with a 6 hour developmental delay. (**E**) Graph comparing the size of wild-type and *eya²* eye discs separated by 6 hours. (**F**) Graph comparing the size of wild-type and *eya²* wing discs at the time at which head capsule genes are beginning to be de-repressed in the eye field. (**G**) Graph comparing the size of wild type and *eya²* adult wings. All *P*-values are listed within supplementary material Table S1. **P*<0.05. Error bars represent s.e.m.

area of wing discs from wild type and *eya*^{2} mutants (*eya* is not expressed in the developing wing). We find that *eya*^{2} wing discs are smaller than their wild-type counterparts at 84-96 hours AEL. This suggests that *eya*^{2} mutant animals are delayed in their development (Fig. 4A-C). We attempted to define the length of the delay and found that the growth of *eya*^{2} animals is slowed by as much as 6 hours (Fig. 4D). Unlike the delays that have been previously reported, the developmental delay that we observe is transitory; there are no statistically significant differences in the size of wing discs by 108 hours AEL or in adult wings (Fig. 4C,G). Furthermore, the timing of eclosion (another measure of global developmental delays) of *eya*^{2} animals is within the time frame that has been established for wild-type flies (data not shown) (Dobzhansky, 1930; Hadorn, 1937). We note that the *eya*^{2} mutant eye discs are still significantly and statistically smaller than their wild-type counterpart even when the 6 hour delay is taken into account (Fig. 4E), indicating that a developmental delay is not the sole cause of the differences in disc size.

De-repression of head capsule selector genes follows cell death in *eya*^{2} mutants

Because developmental cell death in *eya*^{2} mutants is not temporally uniform, we sought to determine whether the de-repression of head capsule selector gene expression precedes, is coincident with or follows the observed wave of apoptosis. We examined the temporal expression pattern of Ct (Fig. 5A-H) and Lim1 (Fig. 5I-P) and find that expanded Ct expression could be observed as early as 84 hours AEL (Fig. 5F, arrow), with the greatest amount of this expansion occurring between 96 and 108 hours AEL (Fig. 5F-H), whereas Lim1 in the eye field is not seen until 108 hours AEL (Fig. 5P, arrow). The time point at which the greatest differences in wing disc size exist (84-96 hours AEL) corresponds to the de-repression of *ct* expression (Fig. 4F). The point at which differences in wing disc sizes are no longer statistically significant (108 hours AEL) corresponds to the establishment of expanded Lim1 expression (Fig. 4C; Fig. 5L,P). Our results support a model in which disruption of the RD network during early larval development results in a wave of developmental cell death and the de-repression of head capsule selector genes in a subset of retinal progenitor and precursor cells. This causes a temporary delay in the growth of other imaginal discs as these cells are now expressing the initial selector genes for two competing GRNs and, thus, two different cell fates. Once the confusion in cell fate choice has been resolved (through the onset of late selector gene expression) and the cells begin adopting a new terminal fate, overall larval development proceeds as expected.

Reduced proliferation levels contribute to the *eya*^{2} small eye disc phenotype

Owing to the change in tissue fate, the smaller size of the *eya*^{2} disc could result from changes in cell proliferation rates. Such a change may reflect differences in the number of cells that are needed to generate a compound eye versus head capsule tissue. It is also possible that the observed decrease in the size of the *eya*^{2} mutant eye disc is due solely to the observed wave of developmental cell death. To determine the relative contribution that cell death plays in regulating the size of the *eya*^{2} disc, we placed p35, an inhibitor of caspase-dependent cell death, under the control of an *ey* retinal enhancer and attempted to block apoptosis in the *eya*^{2} mutant eye disc. In contrast to our expectations, blocking apoptosis did not increase the size of the disc (Fig. 6A,B; supplementary material Fig. S3A,B). In fact, the discs were smaller than the *eya*^{2} control discs (Fig. 6C). This effect is not due to any specific feature of the *eya*^{2} genetic background as forced expression of p35 also decreased the size of the wild-type disc (Fig. 6D). It is unclear why both *eya*^{2} and wild-type eye discs are reduced in size when cell death is blocked. We note, however, that the reduction of wild-type disc size is temporary as the size of the adult eye is not statistically different to that of control flies (supplementary material Fig. S3C-E) (Brumby et al., 2011; Joza et al., 2008).

Cell proliferation rates are reduced in *eya*^{2} mutant discs

To investigate the possibility that alterations in cell proliferation contribute to the *eya*^{2} phenotype, we measured the proliferation rates (number of dividing cells per hour) of wild-type and *eya*^{2} mutant discs using antibodies against pH3, which marks cells that are in late M phase. We find that in wild-type eye discs (between

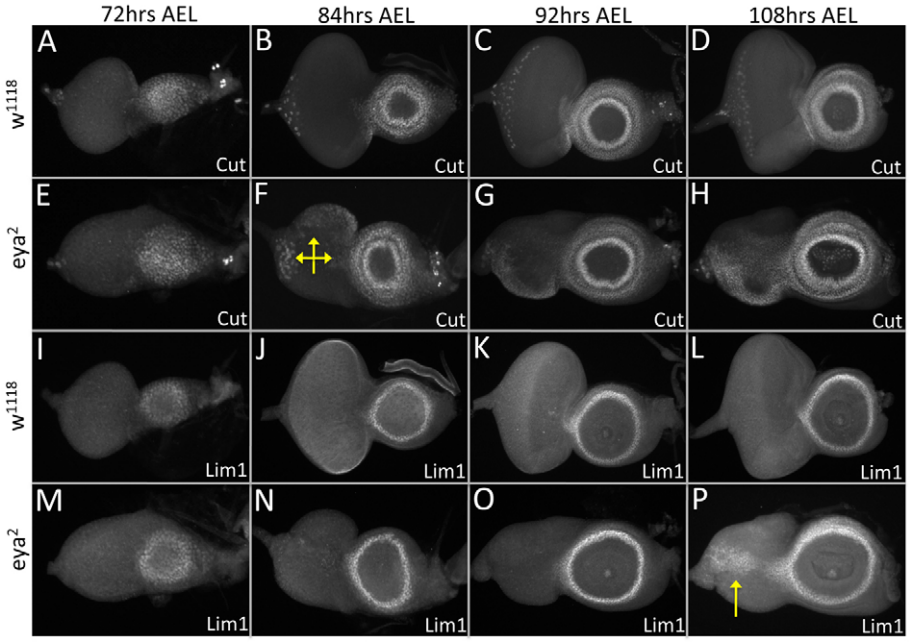

Fig. 5. Developmental time course of head capsule selector gene de-repression. (**A-P**) Confocal images of *Drosophila* third instar eye-antennal discs immunostained for the indicated proteins at different times AEL. Arrows in F and P denote the onset of Cut and Lim1 expression in the eye field.

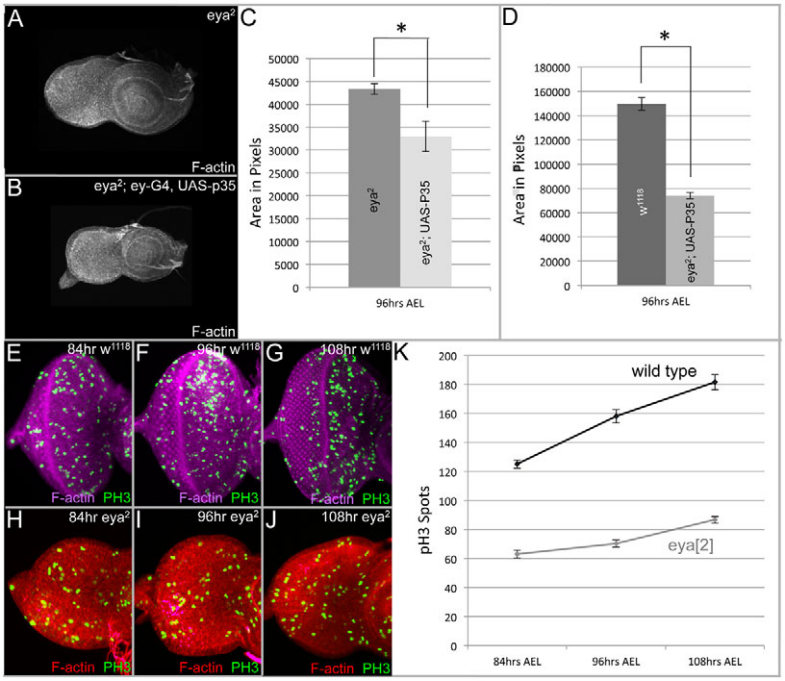

Fig. 6. Reduced proliferation levels contribute to the *eya*^{2} small eye disc phenotype. (**A**,**B**,**E-J**) Confocal images of *Drosophila* third instar eye-antennal discs immunostained for the indicated proteins. (**C**,**D**) Size comparisons of eye discs of different genotypes. (**K**) Cell proliferation rate of wild-type and *eya*^{2} eye fields. All *P*-values are statistically significant and are listed within supplementary material Table S1. **P*<0.05. Error bars represent s.e.m.

84 and 108 hours AEL) cell proliferation rates were nearly twice that of the *eya*^{2} eye disc (Fig. 6E-K). Our results suggest that the small eye disc phenotype is due to the combination of apoptosis and a change in cell proliferation rates. Because *eya*^{2} mutant eye discs continue to increase in size throughout larval development (Fig. 3B), we suggest that the transformation of retinal progenitors and precursors into head capsule directs a change in cell proliferation levels within the former eye field, thereby ensuring that only the appropriate number of cells necessary for an intact head covering are generated. These data indicate that cell fate commitment and cell proliferation are linked processes.

Notch activation restores growth to the *eya*^{2} disc

To determine whether the decrease in proliferation rates observed in *eya*^{2} discs is due to a failure of mutant cells to respond to growth signals, we attempted to increase the size of the eye field either through removal of tumor suppressor genes or through activation of signaling pathways that are known to promote proliferation in the normal eye-antennal disc. Although the mutant discs were unresponsive to some of these signaling pathways (Table 1; Fig. 7D, far right bars), removal of Hippo signaling and activation of the Notch cascade are sufficient to induce growth within the *eya*^{2} disc (Table 1; Fig. 7A-F). We used expression of the retinal precursor *dac* as a readout for determining whether the transformed retinal precursor cells are capable of proliferating in response to Notch signaling. We found that in *eya*^{2} mutant discs 33% of cells express *dac* (Fig. 8A). When Notch is activated in these mutant eye fields the percentage of *dac*-positive cells increases to 59% (Fig. 8A). The increase in *dac* expression is likely to result from a rise in proliferation levels rather than through direct transcriptional regulation of *dac* by the Notch pathway as a subset of Dac-positive cells in the *eya*^{2} disc express the mitotic marker pH3 (Fig. 8B-E; supplementary material Fig. S4C-F) and because forced expression of an activated Notch receptor (N^{icd}) cannot activate *dac* expression in either the *eya*^{2} eye disc (Fig. 8F,G,I, arrow) or wild-type wing discs (supplementary material Fig. S4A,B).

The Notch-mediated increase in the size of the *eya*^{2} disc is not enhanced by the simultaneous inhibition of apoptosis (Fig. 7D). The degree of Notch-dependent proliferation supports our earlier contention that the defect in tissue growth is the major contributor to the small disc phenotype of *eya*^{2} mutants. We further interpret these findings to mean that the transformed head capsule tissue is indeed capable of responding to proliferation signals. In fact, the activation of several cascades, including JAK/STAT and the EGF receptor (EGFR) cascades, resulted in eye-to-antenna transformations (Table 1; data not shown). These results are consistent with an earlier report documenting that manipulation of EGFR and Notch signaling in wild-type discs is sufficient to

Table 1. Activation of Notch signaling or downregulation of the Hippo pathway is sufficient to promote growth in the *eya*^{2} mutant eye field

Pathway	Genetic elements	Growth
Notch	UAS-N^{icd}	+
	UAS-Dl	–
Hedgehog	UAS-hh	–
TGFβ	UAS-dpp	–
	UAS-tkv^{act}	–
JNK	UAS-bsk	–
JAK/STAT	UAS-hop	–
	UAS-upd	*
Hippo	hpo (lof)	+
	UAS-yki	–
	UAS-yki + UAS-sd	–
EGF receptor	UAS-Egfr^{act}	*
	UAS-ras^{V12}	*
RD genes	UAS-tsh	–
	UAS-tio	–
	UAS-eyg	–
	UAS-toe	–
Cell cycle	UAS-string	–
	UAS-cycE	–

+, growth; –, no effect.
*Eye-to-antenna transformation.

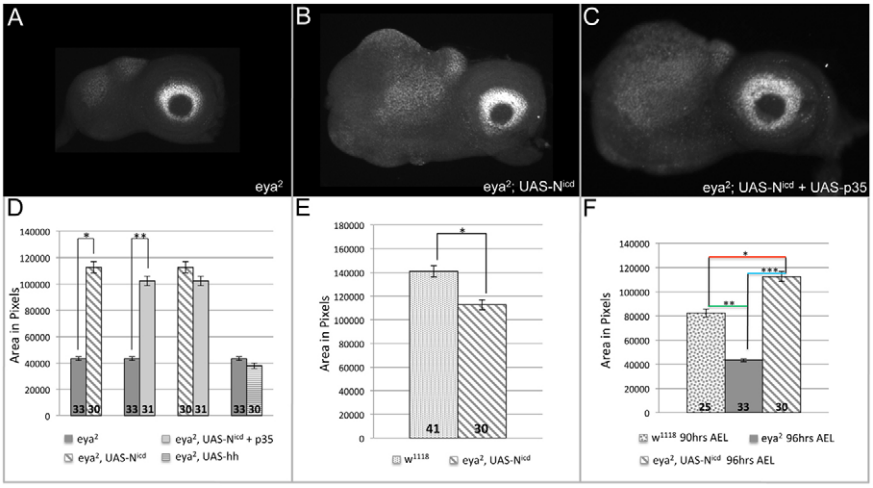

Fig. 7. Activation of Notch signaling restores cell proliferation to *eya²* mutant eye fields. (**A-C**) Confocal images of *Drosophila* third instar eye-antennal discs immunostained for Dachshund at 96 hours AEL. (**D**) Graph comparing the size of the *eya²* eye fields in which Notch signaling has been activated in conjunction with blockade of cell death. (**E**) Graph comparing the size of a wild-type disc to that of the *eya²* mutant in which Notch has been overexpressed. (**F**) Graph incorporating a 6-hour developmental delay into comparisons between the size of wild-type, *eya²* and *eya²*; *UAS-N^{icd}* eye fields. All *P*-values are listed within supplementary material Table S1. **P*<0.05, ***P*<0.05, ****P*<0.05. Error bars represent s.e.m.

transform the eye into an antenna (Kumar and Moses, 2001a). Together, these data suggest that the remaining cells of the *eya²* mutant eye disc are differentially responsive to multiple signaling pathways and that the decrease in proliferation observed in *eya²* mutant eye discs is not is not due to a deficiency in the competency of the cells to respond to proliferation signals.

DISCUSSION

In this article, we have used the eye-antennal disc of *Drosophila* to study the mechanisms by which competing gene regulatory networks (GRNs) impose regional specification upon a naïve tissue. Early in development, the GRNs for the eye, antennal and head capsule fates are uniformly expressed throughout the entire epithelium. During the early/mid second instar stage, the expression and activity of these GRNs are geographically restricted by mechanisms that are poorly understood. Here, we have attempted to determine the mechanism by which this asymmetry is then maintained during the remainder of development. Two competing models can potentially explain the maintenance of asymmetry of GRN expression and activity in an epithelium. In the first model, individual GRNs, once segregated, function primarily to promote the primary fate of the underlying sector. This is achieved solely through internal positive transcriptional feedback loops. In the second model, GRNs not only promote the adoption of primary fates but they also inhibit the implementation of inappropriate fates. This second feature involves GRNs mutually repressing each other's expression.

Many well-defined mutations are known to result in replacement of the eye with head capsule tissue (Hoge, 1915; Milani, 1941; Bonini et al., 1993; Mardon et al., 1994; Curtiss and Heilig, 1995; Curtiss and Heilig, 1997; Royet and Finkelstein, 1997; Jang et al., 2003). Additionally, mutations in which the converse is true have also been characterized, with ectopic eyes forming within portions of the head capsule and antennae (Rauskolb et al., 1995; Pai et al., 1998; Gonzales-Crespo et al., 1995; Pichaud and Casares, 2000; Kumar, 2010). These phenotypes have provided us with an

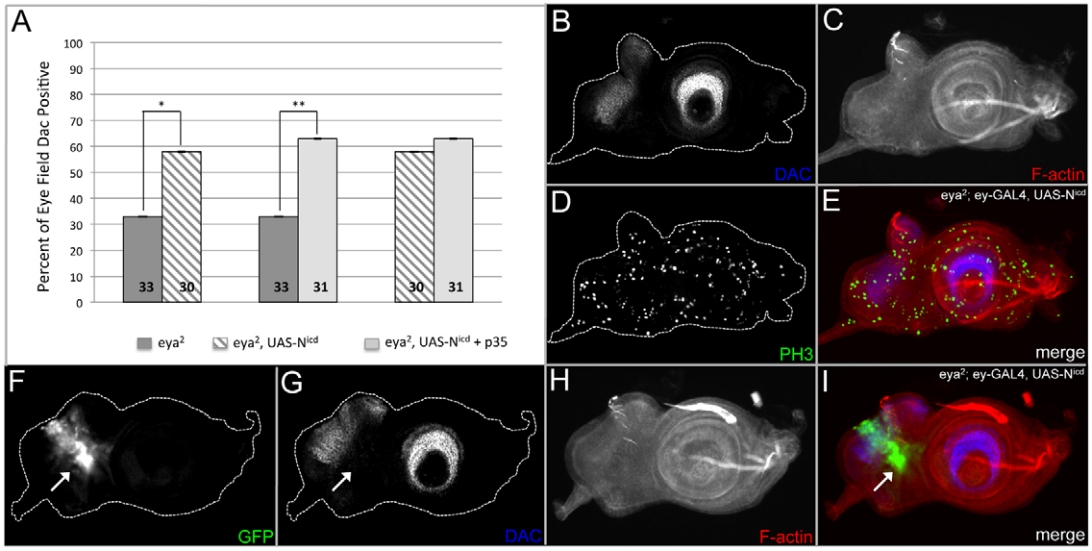

Fig. 8. Activation of Notch signaling stimulates growth of the *eya²* disc. (**A**) Graph comparing the percentage of the wild-type and mutant eye fields containing Dac protein. All *P*-values are listed within supplementary material Table S1. **P*<0.05, ***P*<0.05. Error bars represent s.e.m. (**B-I**) Confocal images of third instar eye-antennal discs immunostained for the indicated proteins. White arrows indicate areas where Notch signaling does not activate Dac expression. Dotted lines delineate the outline of the eye-antennal disc.

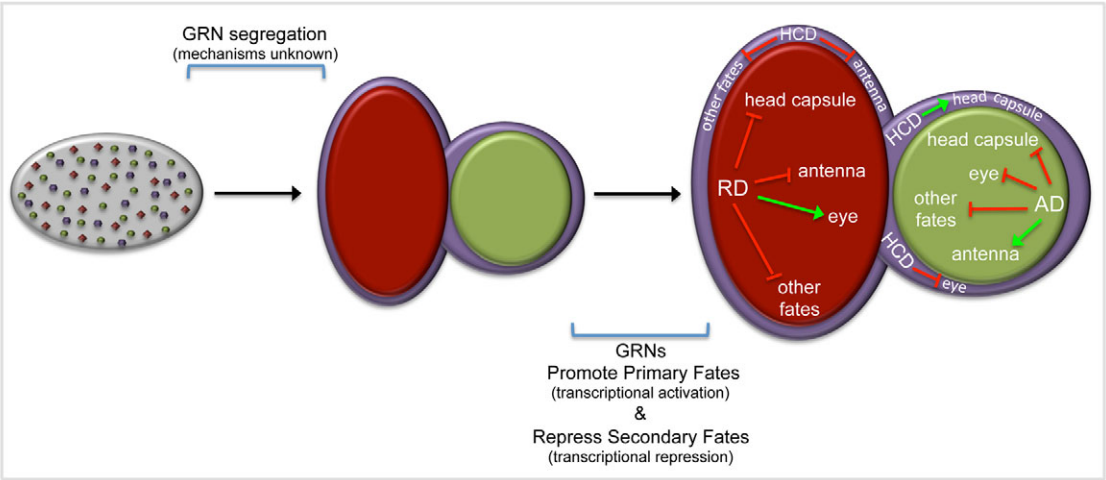

Fig. 9. Model for regional specification in the eye-antennal disc of *Drosophila*. Early in development, GRNs for multiple fates are co-expressed throughout the entire eye-antennal field. Via poorly understood mechanisms these GRNs are geographically separated. Each GRN must promote its primary fate via transcriptional activation while inhibiting alternative fates via transcriptional repression of other GRNs. AD, antennal determination; HCD, head capsule determination.

opportunity to elucidate the mechanisms that underlie regional specification. Here, we present evidence that mutual repression of GRN expression patterns plays an important role in this process. We re-analyzed the fate of the eye field in *eya* and *so* loss-of-function mutants and find that a subpopulation of retinal progenitor and precursor cells is transformed into head capsule tissue. These cells survive an apoptotic wave of developmental cell death, activate expression of head capsule genes and re-adjust their cell proliferation rates to match their newly acquired identity. These results suggest that one function of the RD network is to repress the expression of non-retinal selector genes. Although the execution of this task has been attributed to Ey (Kenyon et al., 2003), increasing evidence suggests that the repression of non-retinal selector genes is more likely to be a function of the So-Eya complex (this report) (Anderson et al., 2012; Wang and Sun, 2012). Currently, it is unclear whether So binds to tissue-specific enhancers of non-retinal selector genes and directly represses transcription. However, such a mechanism is possible as So consensus binding sites are found within several of these transcription units (determined by FlyEnhancer searching software) (Pauli et al., 2005).

If competition among GRNs is important for ensuring regional specification then what is the critical developmental window for this event to take place? Previous published reports indicate that many members of the eye, antennal and head capsule GRNs are uniformly expressed throughout the entire eye-antennal disc primordium during embryogenesis and the first larval instar (Quiring et al., 1994; Royet and Finkelstein, 1997; Czerny et al., 1999; Kumar and Moses, 2001b; Jang et al., 2003; Aldaz et al., 2003). Other studies have indicated that by the late second larval instar these genes are geographically segregated within the eye-antennal disc (Kumar and Moses, 2001a; Kenyon et al., 2003). If a phenocritical period does exist for regional specification within the eye-antennal disc, then one would predict that the fate of the eye field could be altered during this developmental window under circumstances in which the eye GRN is compromised. Indeed, alterations in both EGF receptor and Notch signaling do indeed result in the transformation of the eye into an antenna during the second larval instar (Kumar and Moses, 2001a). In this article, we demonstrate a similar phenomenon: compromising the function of the retinal determination network leads to the transformation of the eye into head capsule tissue. This transformation is initiated between 84 and 96 hours AEL as genes that are normally restricted to the developing head capsule are de-repressed within the eye field of both *eya* and *so* mutants. If one accounts for differences in the experimental temperatures at which this study and that of Kumar and Moses were conducted then the phenocritical windows for eye–antenna-and-eye–head capsule transformations map to very similar time periods.

We propose that our model for the use of transcriptional repression by GRNs to promote regional specification is applicable to the formation of the antenna and head capsule as well because forced expression of *ct* within the eye field extinguishes *ey* expression and induces eye-antenna transformations (Duong et al., 2008; Anderson et al., 2012). Similarly, forced expression of Dip3 within the eye field is sufficient to simultaneously downregulate the RD network while ectopically activating antennal selector genes such as Distal-less (Dll) thereby resulting in eye-antennal transformations (Duong et al., 2008). This result indicates that the GRNs for antennal and head capsule tissue can inhibit expression of genes within the RD network. Our identification of a potential phenocritical period for the eye-head capsule choice might be relevant to other tissue fate decisions as well. For instance, the critical window for the wing-notum decision has been mapped to the late second instar (Baonza et al., 2000), and the induction of ectopic eyes (non-retinal to retinal transformation) appears in most instances to be synchronous with the specification of the normal eye (Salzer and Kumar, 2010). Together, these results suggest that a potential global developmental window for imaginal disc fate decisions exists and is centered around the late second larval/early third instar stage.

In summary, we propose that during the earliest stages of normal eye-antennal disc development the members of multiple GRNs are expressed uniformly throughout the epithelium (Fig. 9, left). As development proceeds, each GRN is geographically restricted (Fig. 9, middle). The maintenance of these transcriptional asymmetries is maintained by a combination of intra-GRN activation and inter-GRN repression (Fig. 9, right). In situations in which the retinal determination network is compromised, the antennal and head

capsule GRNs are de-repressed within the eye field. The choice of which developmental pathway is to be activated depends heavily upon the type of genetic manipulation. Likewise, when an individual retinal determination gene such as *ey* is forcibly expressed in a non-retinal tissue it simultaneously activates the rest of the RD network while repressing expression of the endogenous GRN. As a result, an ectopic eye is generated.

Acknowledgements
We thank members of the Kumar lab for comments on the manuscript as well as Georg Halder, Bruce Hay, Ross Cagan, Marc Muskavitsch, Jessica Treisman, Phil Beachy, Erika Bach, Duojia Pan, Laurent Fasano, Albert Courey, Francesca Pignoni, Fernando Casares, Richard Mann, Tiffany Cook, Juan Botas, the Developmental Studies Hybridoma Bank and the Bloomington *Drosophila* Stock Center for gifts of fly strains and antibodies.

Funding
This work is supported by a grant from the National Eye Institute [2R01 EY014863 to J.P.K.]. Deposited in PMC for release after 12 months.

Competing interests statement
The authors declare no competing financial interests.

Supplementary material
Supplementary material available online at
http://dev.biologists.org/lookup/suppl/doi:10.1242/dev.085423/-/DC1

References

Aldaz, S., Morata, G. and Azpiazu, N. (2003). The Pax-homeobox gene eyegone is involved in the subdivision of the thorax of Drosophila. *Development* **130**, 4473-4482.
Anderson, A. M., Weasener, B. M., Weasner, B. P. and Kumar, J. P. (2012). Dual transcriptional activities of SIX proteins define their roles in normal and ectopic eye development. *Development* **139**, 991-1000.
Baker, W. K. (1978). A fine-structure gynandromorph fate map of the Drosophila head. *Genetics* **88**, 743-754.
Baonza, A. and Freeman, M. (2002). Control of Drosophila eye specification by Wingless signalling. *Development* **129**, 5313-5322.
Baonza, A., Roch, F. and Martin-Blanco, E. (2000). DER signaling restricts the boundaries of the wing field during Drosophila development. *Proc. Natl. Acad. Sci. USA* **97**, 7331-7335.
Bessa, J., Gebelein, B., Pichaud, F., Casares, F. and Mann, R. S. (2002). Combinatorial control of Drosophila eye development by eyeless, homothorax, and teashirt. *Genes Dev.* **16**, 2415-2427.
Blanco, J., Seimiya, M., Pauli, T., Reichert, H. and Gehring, W. J. (2009). Wingless and Hedgehog signaling pathways regulate orthodenticle and eyes absent during ocelli development in Drosophila. *Dev. Biol.* **329**, 104-115.
Blochlinger, K., Jan, L. Y. and Jan, Y. N. (1993). Postembryonic patterns of expression of cut, a locus regulating sensory organ identity in Drosophila. *Development* **117**, 441-450.
Bodmer, R., Barbel, S., Sheperd, S., Jack, J. W., Jan, L. Y. and Jan, Y. N. (1987). Transformation of sensory organs by mutations of the cut locus of D. melanogaster. *Cell* **51**, 293-307.
Bonini, N. M., Leiserson, W. M. and Benzer, S. (1993). The eyes absent gene: genetic control of cell survival and differentiation in the developing Drosophila eye. *Cell* **72**, 379-395.
Brumby, A. M., Goulding, K. R., Schlosser, T., Loi, S., Galea, R., Khoo, P., Bolden, J. E., Aigaki, T., Humbert, P. O. and Richardson, H. E. (2011). Identification of novel Ras-cooperating oncogenes in Drosophila melanogaster: a RhoGEF/Rho-family/JNK pathway is a central driver of tumorigenesis. *Genetics* **188**, 105-125.
Bui, Q. T., Zimmerman, J. E., Liu, H., Gray-Board, G. L. and Bonini, N. M. (2000). Functional analysis of an eye enhancer of the Drosophila eyes absent gene: differential regulation by eye specification genes. *Dev. Biol.* **221**, 355-364.
Callaerts, P., Halder, G. and Gehring, W. J. (1997). PAX-6 in development and evolution. *Annu. Rev. Neurosci.* **20**, 483-532.
Chen, R., Amoui, M., Zhang, Z. and Mardon, G. (1997). Dachshund and eyes absent proteins form a complex and function synergistically to induce ectopic eye development in Drosophila. *Cell* **91**, 893-903.
Cheyette, B. N., Green, P. J., Martin, K., Garren, H., Hartenstein, V. and Zipursky, S. L. (1994). The Drosophila sine oculis locus encodes a homeodomain-containing protein required for the development of the entire visual system. *Neuron* **12**, 977-996.
Cordero, J. B. and Cagan, R. L. (2010). Canonical wingless signaling regulates cone cell specification in the Drosophila retina. *Dev. Dyn.* **239**, 875-884.
Cordero, J. B., Jassim, O., Bao, S. and Cagan, R. (2004). A role for wingless in an early pupal cell death event that contributes to patterning the Drosophila eye. *Mech. Dev.* **121**, 1523-1530.
Curtiss, J. and Heilig, J. S. (1995). Establishment of Drosophila imaginal precursor cells is controlled by the Arrowhead gene. *Development* **121**, 3819-3828.
Curtiss, J. and Heilig, J. S. (1997). Arrowhead encodes a LIM homeodomain protein that distinguishes subsets of Drosophila imaginal cells. *Dev. Biol.* **190**, 129-141.
Czerny, T., Halder, G., Kloter, U., Souabni, A., Gehring, W. J. and Busslinger, M. (1999). twin of eyeless, a second Pax-6 gene of Drosophila, acts upstream of eyeless in the control of eye development. *Mol. Cell* **3**, 297-307.
Davidson, E. H. and Levine, M. S. (2008). Properties of developmental gene regulatory networks. *Proc. Natl. Acad. Sci. USA* **105**, 20063-20066.
Duong, H. A., Wang, C. W., Sun, Y. H. and Courey, A. J. (2008). Transformation of the eye to antenna by misexpression of a single gene. *Mech. Dev.* **125**, 130-141.
Dobzhansky, T. (1930). Time of development of the different sexual forms in *Drosophila melanogaster. Biol. Bull.* **59**, 128-133.
Ferris, G. F. (1950). External morphoogy of the adult. In *Biology of Drosophila* (ed. M. Demerec), pp. 368-419. New York, NY: J. Wiley.
Gehring, W. (1966). Cell heredity and changes of determination in cultures of imaginal discs in Drosophila melanogaster. *J. Embryol. Exp. Morphol.* **15**, 77-111.
González-Crespo, S. and Morata, G. (1995). Control of Drosophila adult pattern by extradenticle. *Development* **121**, 2117-2125.
Hadorn, E. (1937). An accelerating effect of normal "ring-glands" on puparium-formation in lethal larvae of *Drosophila melanogaster. Proc. Natl. Acad. Sci. USA* **23**, 478-484.
Halder, G., Callaerts, P. and Gehring, W. J. (1995). New perspectives on eye evolution. *Curr. Opin. Genet. Dev.* **5**, 602-609.
Halder, G., Callaerts, P., Flister, S., Walldorf, U., Kloter, U. and Gehring, W. J. (1998). Eyeless initiates the expression of both sine oculis and eyes absent during Drosophila compound eye development. *Development* **125**, 2181-2191.
Haynie, J. L. and Bryant, P. J. (1986). Development of the eye-antenna imaginal disc and morphogenesis of the adult head in Drosophila melanogaster. *J. Exp. Zool.* **237**, 293-308.
Hazelett, D. J., Bourouis, M., Walldorf, U. and Treisman, J. E. (1998). decapentaplegic and wingless are regulated by eyes absent and eyegone and interact to direct the pattern of retinal differentiation in the eye disc. *Development* **125**, 3741-3751.
Hoge, M. A. (1915). Another gene in the fourth chromosome of Drosophila. *Am. Nat.* **49**, 47-49.
Hussey, R. G., Thompson, W. R. and Calhoun, E. T. (1927). The influence of X-rays on the development of Drosophila larvae. *Science* **66**, 65-66.
Jang, C. C., Chao, J. L., Jones, N., Yao, L. C., Bessarab, D. A., Kuo, Y. M., Jun, S., Desplan, C., Beckendorf, S. K. and Sun, Y. H. (2003). Two Pax genes, eye gone and eyeless, act cooperatively in promoting Drosophila eye development. *Development* **130**, 2939-2951.
Joza, N., Galindo, K., Pospisilik, J. A., Benit, P., Rangachari, M., Kanitz, E. E., Nakashima, Y., Neely, G. G., Rustin, P., Abrams, J. M. et al. (2008). The molecular archaeology of a mitochondrial death effector: AIF in Drosophila. *Cell Death Differ.* **15**, 1009-1018.
Kenyon, K. L., Ranade, S. S., Curtiss, J., Mlodzik, M. and Pignoni, F. (2003). Coordinating proliferation and tissue specification to promote regional identity in the Drosophila head. *Dev. Cell* **5**, 403-414.
Kumar, J. P. (2010). Retinal determination the beginning of eye development. *Curr. Top. Dev. Biol.* **93**, 1-28.
Kumar, J. P. and Moses, K. (2001a). EGF receptor and Notch signaling act upstream of Eyeless/Pax6 to control eye specification. *Cell* **104**, 687-697.
Kumar, J. P. and Moses, K. (2001b). Expression of evolutionarily conserved eye specification genes during Drosophila embryogenesis. *Dev. Genes Evol.* **211**, 406-414.
Lebovitz, R. M. and Ready, D. F. (1986). Ommatidial development in Drosophila eye disc fragments. *Dev. Biol.* **117**, 663-671.
Lim, H. Y. and Tomlinson, A. (2006). Organization of the peripheral fly eye: the roles of Snail family transcription factors in peripheral retinal apoptosis. *Development* **133**, 3529-3537.
Lin, H. V., Rogulja, A. and Cadigan, K. M. (2004). Wingless eliminates ommatidia from the edge of the developing eye through activation of apoptosis. *Development* **131**, 2409-2418.
Lopes, C. S. and Casares, F. (2010). hth maintains the pool of eye progenitors and its downregulation by Dpp and Hh couples retinal fate acquisition with cell cycle exit. *Dev. Biol.* **339**, 78-88.
Ma, C. and Moses, K. (1995). Wingless and patched are negative regulators of the morphogenetic furrow and can affect tissue polarity in the developing Drosophila compound eye. *Development* **121**, 2279-2289.
Madhaven, M. M. and Schneiderman, H. A. (1977). Histological analysis of the dynamics of growth of imaginal discs and histoblast nests during the larval development of *Drosophila melanogaster. Dev. Genes Evol.* **183**, 269-305.

Mardon, G., Solomon, N. M. and Rubin, G. M. (1994). dachshund encodes a nuclear protein required for normal eye and leg development in Drosophila. *Development* **120**, 3473-3486.
Milani, R. (1941). Two new eye-shape mutant alleles in *Drosophila melanogaster. DIS* **14**, 52.
Nicholson, S. C., Gilbert, M. M., Nicolay, B. N., Frolov, M. V. and Moberg, K. H. (2009). The archipelago tumor suppressor gene limits rb/e2f-regulated apoptosis in development Drosophila tissues. *Curr. Biol.* **19**, 1503-1510.
Niimi, T., Seimiya, M., Kloter, U., Flister, S. and Gehring, W. J. (1999). Direct regulatory interaction of the eyeless protein with an eye-specific enhancer in the sine oculis gene during eye induction in Drosophila. *Development* **126**, 2253-2260.
Ostrin, E. J., Li, Y., Hoffman, K., Liu, J., Wang, K., Zhang, L., Mardon, G. and Chen, R. (2006). Genome-wide identification of direct targets of the Drosophila retinal determination protein Eyeless. *Genome Res.* **16**, 466-476.
Ouweneel, W. J. (1970). Normal and abnormal determination in the imaginal discs of Drosophila, with special reference to the eye discs. *Acta Embryol. Exp. (Palermo)* **1**, 95-119.
Pai, C. Y., Kuo, T. S., Jaw, T. J., Kurant, E., Chen, C. T., Bessarab, D. A., Salzberg, A. and Sun, Y. H. (1998). The Homothorax homeoprotein activates the nuclear localization of another homeoprotein, extradenticle, and suppresses eye development in Drosophila. *Genes Dev.* **12**, 435-446.
Pauli, T., Seimiya, M., Blanco, J. and Gehring, W. J. (2005). Identification of functional sine oculis motifs in the autoregulatory element of its own gene, in the eyeless enhancer and in the signalling gene hedgehog. *Development* **132**, 2771-2782.
Peng, H. W., Slattery, M. and Mann, R. S. (2009). Transcription factor choice in the Hippo signaling pathway: homothorax and yorkie regulation of the microRNA bantam in the progenitor domain of the Drosophila eye imaginal disc. *Genes Dev.* **23**, 2307-2319.
Pichaud, F. and Casares, F. (2000). homothorax and iroquois-C genes are required for the establishment of territories within the developing eye disc. *Mech. Dev.* **96**, 15-25.
Pignoni, F., Hu, B., Zavitz, K. H., Xiao, J., Garrity, P. A. and Zipursky, S. L. (1997). The eye-specification proteins So and Eya form a complex and regulate multiple steps in Drosophila eye development. *Cell* **91**, 881-891.
Quiring, R., Walldorf, U., Kloter, U. and Gehring, W. J. (1994). Homology of the eyeless gene of Drosophila to the Small eye gene in mice and Aniridia in humans. *Science* **265**, 785-789.
Rauskolb, C., Smith, K. M., Peifer, M. and Wieschaus, E. (1995). extradenticle determines segmental identities throughout Drosophila development. *Development* **121**, 3663-3673.
Roignant, J. Y., Legent, K., Janody, F. and Treisman, J. E. (2010). The transcriptional co-factor Chip acts with LIM-homeodomain proteins to set the boundary of the eye field in Drosophila. *Development* **137**, 273-281.
Royet, J. and Finkelstein, R. (1995). Pattern formation in Drosophila head development: the role of the orthodenticle homeobox gene. *Development* **121**, 3561-3572.
Royet, J. and Finkelstein, R. (1996). Hedgehog, wingless and orthodenticle specify adult head development in Drosophila. *Development* **122**, 1849-1858.
Royet, J. and Finkelstein, R. (1997). Establishing primordia in the Drosophila eye-antennal imaginal disc: the roles of decapentaplegic, wingless and hedgehog. *Development* **124**, 4793-4800.
Salzer, C. L. and Kumar, J. P. (2009). Position dependent responses to discontinuities in the retinal determination network. *Dev. Biol.* **326**, 121-130.
Salzer, C. L. and Kumar, J. P. (2010). Identification of retinal transformation hot spots in developing Drosophila epithelia. *PLoS ONE* **5**, e8510.
Serikaku, M. A. and O'Tousa, J. E. (1994). Sine oculis is a homeobox gene required for Drosophila visual system development. *Genetics* **138**, 1137-1150.
Simpson, P., Berreur, P. and Berreur-Bonnenfant, J. (1980). The intitiation of pupariation in Drosophila: dependence on growth of the imaginal discs. *J. Embryol. Exp. Morphol.* **57**, 566-571.
Smith-Bolton, R. K., Worley, M. I., Kanda, H. and Hariharan, I. K. (2009). Regenerative growth in Drosophila imaginal discs is regulated by Wingless and Myc. *Dev. Cell* **16**, 797-809.
Tahayato, A., Sonneville, R., Pichaud, F., Wernet, M. F., Papatsenko, D., Beaufils, P., Cook, T. and Desplan, C. (2003). Otd/Crx, a dual regulator for the specification of ommatidia subtypes in the Drosophila retina. *Dev. Cell* **5**, 391-402.
Tomlinson, A. (2003). Patterning the peripheral retina of the fly: decoding a gradient. *Dev. Cell* **5**, 799-809.
Treisman, J. E. and Rubin, G. M. (1995). Wingless inhibits morphogenetic furrow movement in the Drosophila eye disc. *Development* **121**, 3519-3527.
Tsuji, T., Sato, A., Hiratani, I., Taira, M., Saigo, K. and Kojima, T. (2000). Requirement of Lim1, a Drosophila, LIM-homeobox gene, for normal leg and antennal development. *Development* **127**, 4315-4323.
Vogt, M. (1946). Zur labilen Determination der Imagin-alscheiben von Drosophila. I. Verhalten verschieden-altriger Imaginalanlagen bei operativer Defektsetzung. *Biol. Zbl.* **65**, 223-238.
Wang, C. W. and Sun, Y. H. (2012). Segregation of eye and antenna fates maintained by mutual antagonism in Drosophila. *Development* **139**, 3413-3421.

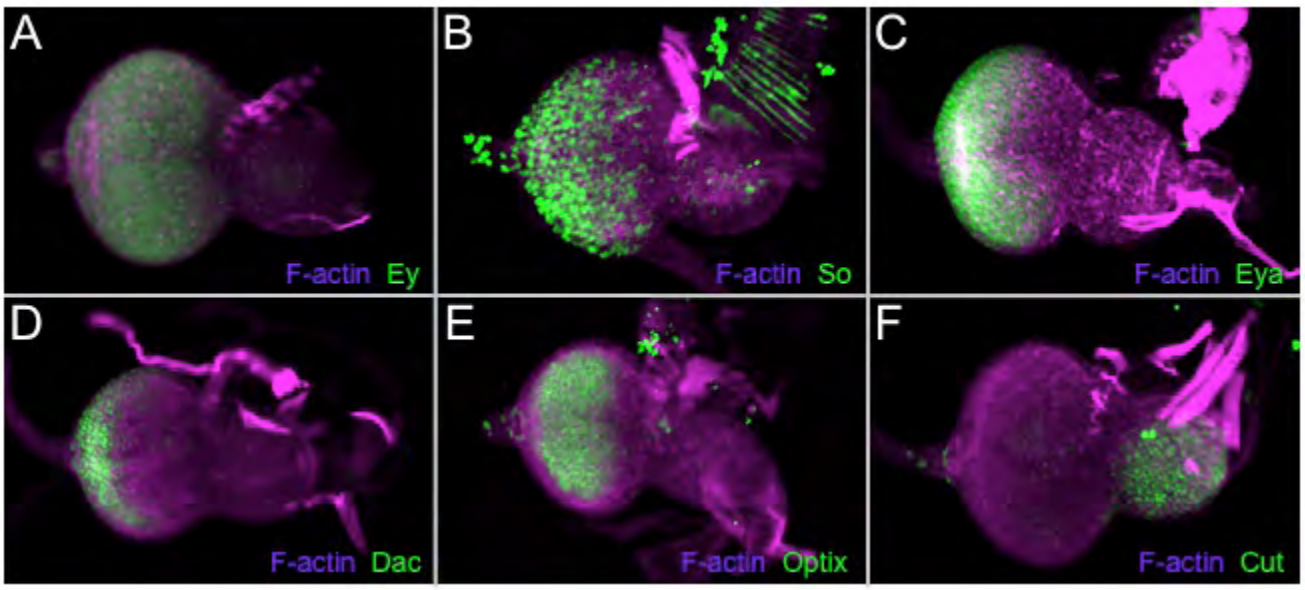

Fig. S1. Selector genes are segregated within the eye and antenna by 72 hours AEL. (**A-F**) Confocal images of 72 hour AEL wild-type eye-antennal discs. Detected proteins are listed within the figure. Anterior is to the right.

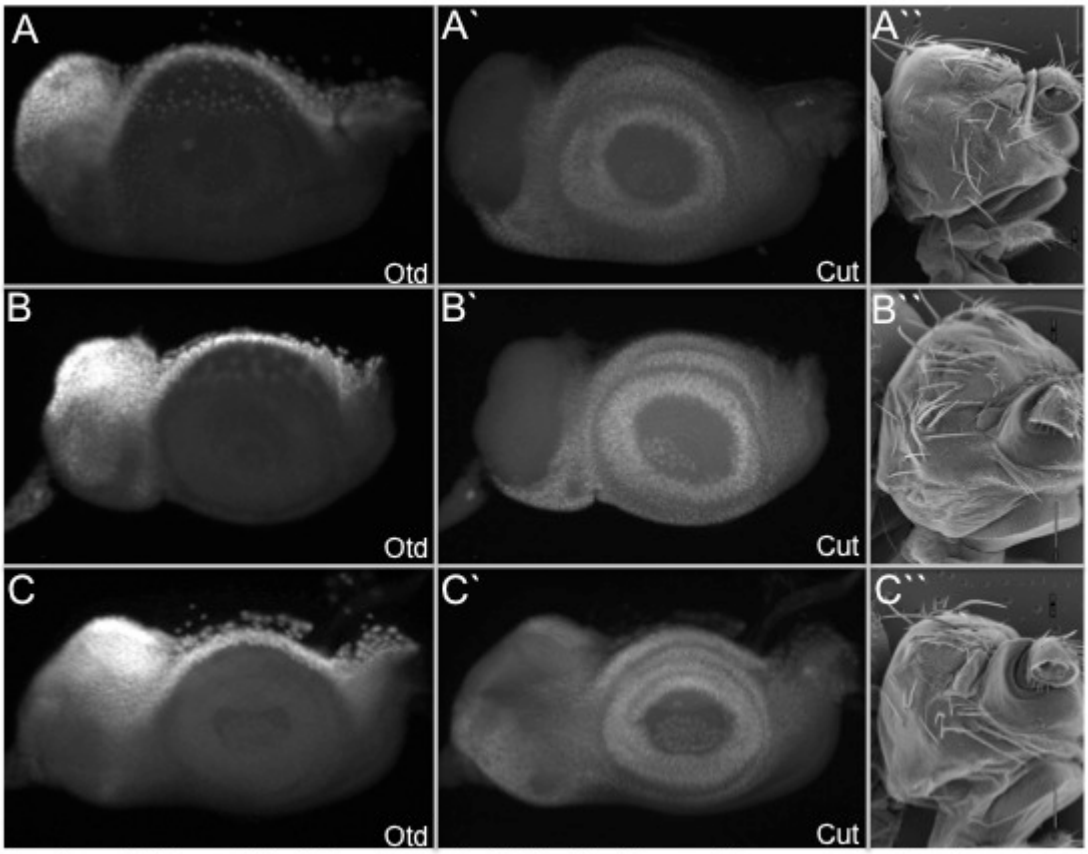

Fig. S2. Variable patterns of adult head cuticle result from non-stereotyped gene expression patterns. (**A-C**,**A′-C′**) Confocal images of *eya*^{2} mutant third instar eye-antennal discs. Detected proteins are listed within the figure. Note the variability in the expression patterns of both Otd and Cut. Anterior is to the right. (**A″-C″**) Scanning electron micrographs of adult *eya*^{2} heads. Note the variability in the head cuticle patterns in the adult heads.

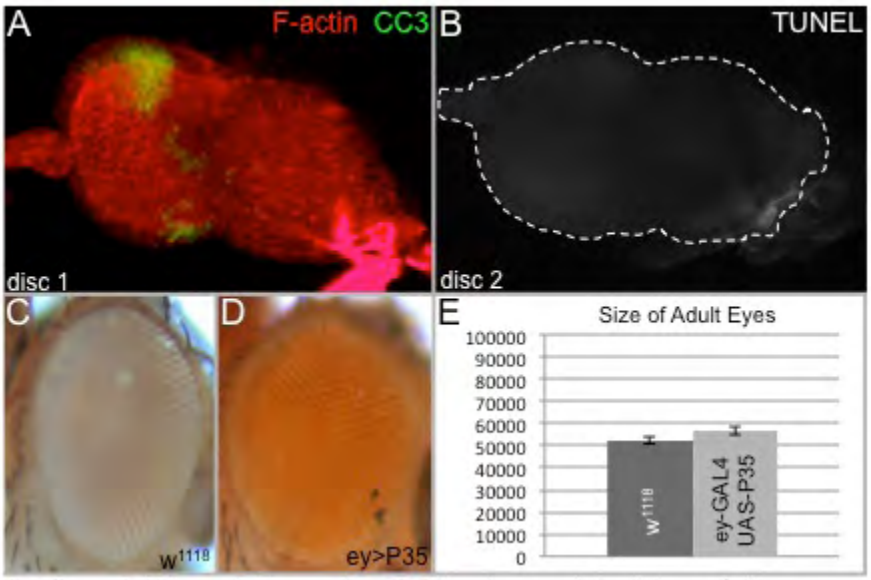

Fig. S3. Expression of p35 reduces cell death in *eya*^{2} discs. (**A**,**B**) Confocal images of third instar *eya*^{2} eye-antennal discs. (A) Expression of p35 in the eye field alters the localization of cleaved caspase-3, which is now segregated to the membrane. This is consistent with previous descriptions of p35 activity. (B). Expression of p35 reduces the number of dying cells. In this image, the level of TUNEL staining is dramatically reduced (compare with the level of CC3 staining in Fig. 3G,H). (**C**,**D**) Light microscope images of adult wild-type and ey-GAL4, UAS-P35 eyes. (**E**) Size comparison of wild-type and ey-GAL4, UAS-P35 adult eyes (area). Detected proteins are listed within the figure. Anterior is to the right. Error bars represent s.e.m.

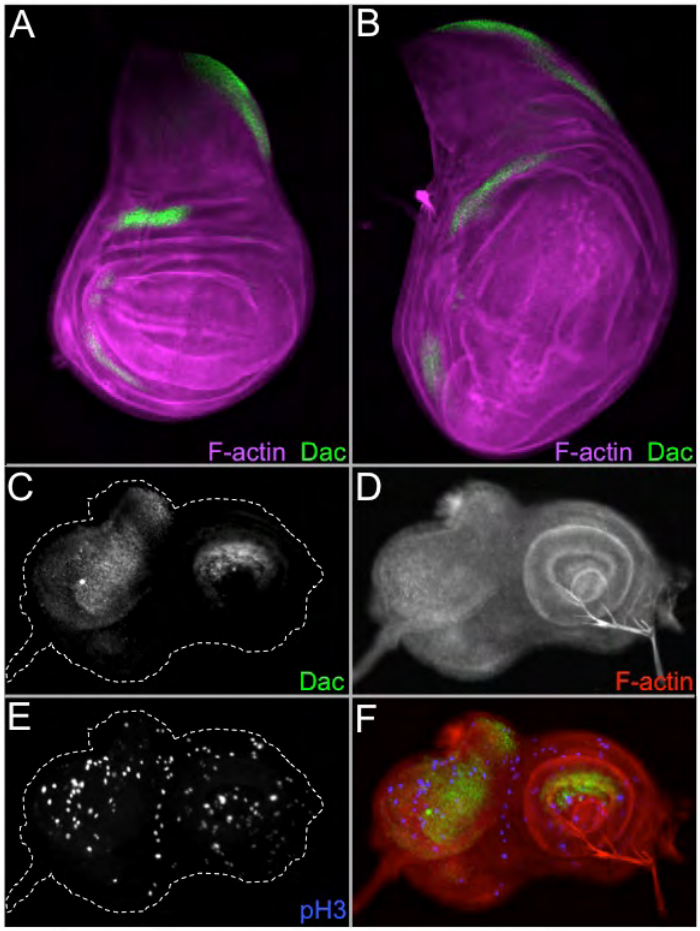

Fig. S4. Notch signaling does not directly activate *dac* expression in the eye and wing disc. (**A**,**B**) Confocal images of third instar wing discs. (A) Distribution of Dac protein in wild type. (B) Expression of N^{icd} along the A/P axis with dpp-GAL4 does not activate ectopic *dac* expression. Note the increased size of the wing disc in response to Notch signaling. (**C-F**) Confocal images of third instar *eya*^{2} eye-antennal discs. Note that several *dac*-positive cells (green) are also pH3 positive (blue), suggesting that at this point in development at least some retinal precursors proliferate in response to Notch signaling. Detected proteins are listed within the figure. Anterior is to the right.

Table S1. *P*-values for growth studies

Figure	Description	*P*-value
Fig. 3A	**Time point**	
	72 hours AEL	0.001
	84 hours AEL	1.99E-39
	96 hours AEL	2.60E-31
	108 hours AEL	9.44E-30
Fig. 3B	**Time point comparison**	
	72/84 hours AEL	0.0003
	84/96 hours AEL	5.80E-20
	96/108 hours AEL	1.30E-15
Fig. 4C	**Time point**	
	84 hours AEL	0.0002
	90 hours AEL	2.80E-06
	96 hours AEL	3.69E-15
	102 hours AEL	0.0084
	108 hours AEL	0.07
Fig. 4D	**Time point comparison**	
	w^{1118} 84 hours /eya^2 90 hours	4.46E-07
	w^{1118} 90 hours /eya^2 96 hours	0.77
	w^{1118} 96 hours /eya^2 102 hours	0.003
	w^{1118} 102 hours /eya^2 108 hours	0.06
Fig. 4E	**Asterisk/Genotype comparison**	
	* w^{1118} 90 hours /eya^2 96 hours	1.30E-12
Fig. 4F	**Asterisk/Genotype comparison**	
	* w^{1118} 96 hours /eya^2 96 hours	3.69E-15
Fig. 4G		
	wild type vs eya[2]	0.574
Fig. 6C	**Asterisk/Time point**	
	96 hours AEL	0.008
Fig. 6D	**Asterisk/Time point**	
	96 hours AEL	1.03E-18
Fig. 7D	**Genotype comparison**	
	eya^2/eya^2, UAS-N^{icd}	1.90E-12

	eya^2/ eya^2, UAS-N^{icd}+p35	4.45E-16
	eya^2, UAS-N^{icd}/eya^2, UAS-N^{icd} +p35	0.07
	eya^2/eya^2, UAS-hh	0.08
Fig. 7E	**Genotype comparison**	
	w^{1118}/eya^2, UAS-N^{icd} 96 hours AEL	1.32E-06
Fig. 7F	**Asterisk/Genotype comparison**	
	* w^{1118} 90 hours /eya^2, UAS-N^{icd} 96 hours	1.06E-06
	** w^{1118} 90hr/eya^2 96hr	1.29E-12
	*** eya^2 96 hours /eya^2, UAS-N^{icd} 96 hours	5.04E-17
Fig. 8A	**Asterisk/Genotype comparison**	
	* eya^2/eya^2, UAS-N^{icd}	1.90E-12
	** eya^2/eya^2, UAS-N^{icd} +p35	6.80E-12
	eya^2, UAS-N^{icd}/eya^2, UAS-N^{icd} +p35	0.34